Evolution, 2023, **77(4)**, 1006–1018
https://doi.org/10.1093/evolut/qpad020
Advance access publication 13 February 2023
Original Article

OXFORD

Multilevel analysis of integration and disparity in the mammalian skull

Emma Sherratt[1] and Brian Kraatz[2]

[1]School of Biological Sciences, The University of Adelaide, Adelaide, SA, Australia
[2]Department of Anatomy, Western University of Health Sciences, Pomona, CA, United States
Corresponding author: North Terrace, School of Biological Sciences, The University of Adelaide, SA 5005, Australia. Email: emma.sherratt@gmail.com

Abstract

Biological variation is often considered in a scalable hierarchy, e.g., within the individual, within the populations, above the species level. Morphological integration, the concept of covariation among constituent parts of an organism, is also hierarchical; the degree to which these "modules" covary is a matter of the scale of the study as well as underlying processes driving the covariation. Multilevel analyses of trait covariation are a valuable tool to infer the origins and historical persistence of morphological diversity. Here, we investigate concordance in patterns of integration and modularity across three biological levels of variation: within a species, within two genera-level radiations, and among species at the family level. We demonstrate this approach using the skull of mammalian family Leporidae (rabbits and hares), which is morphologically diverse and has a rare-among-mammals functional signal of locomotion adaptation. We tested three alternative hypotheses of modularity; from the most supported we investigated disparity and integration of each module to infer which is most responsible for patterns of cranial variation across these levels, and whether variation is partitioned consistently across levels. We found a common pattern of modularity underlies leporid cranial diversity, though there is inconsistency across levels in each module's disparity and integration. The face module contributes the most to disparity at all levels, which we propose is facilitating evolutionary diversity in this clade. Therefore, the distinctive facial tilt of leporids is an adaptation to locomotory behavior facilitated by a modular system that allows lineages to respond differently to selection pressures.

Keywords: morphological integration, modularity, skull, geometric morphometrics

Introduction

A long-standing question in evolutionary biology pertains to whether patterns of macroevolution are the result of successive iterations of microevolution (Erwin, 2000; Hansen & Martins, 1996; Lande, 1980). This notion of a scalable, hierarchical biological variation has for decades been examined with respect to predictable morphological changes with body size; the most common conclusion is that ontogenetic allometry leads to static allometry, which underlies evolutionary allometry (Cock, 1966; Cheverud, 1982b; Klingenberg, 1996). Testing this with real datasets has allowed researchers to understand evolvability and infer the processes generating diversity (e.g., Klingenberg, 1992; Leamy & Atchley, 1984; Marcy et al., 2020; Pelabon et al., 2014; Voje et al., 2014). Morphological integration (sensu Olson & Miller, 1958) also occurs across a hierarchy of biological levels (Klingenberg, 2014; Zelditch & Goswami, 2021) and has the potential to be scalable. Morphological integration at each level may arise from distinct mechanisms, which may leave distinct signals identifiable through morphometric correlations and could help to infer the processes involved in its generation. Yet correlations at one level, may structure the correlations observed at the next successive level. Thus multilevel analyses are a valuable tool to test this (Klingenberg, 2014); analyzing integration at different taxonomic levels within diverse radiations provides an opportunity to understand whether the processes responsible for variation within a species may also facilitate adaptive variation among species (Benítez et al., 2022; Monteiro & Nogueira, 2010; Monteiro et al., 2005; Urošević et al., 2018; Young & Badyaev, 2006). Despite the value of multilevel study of morphological variation and integration, they remain relatively uncommon.

The skull is a well-studied structure from the perspective of morphological integration, and predicted to be composed of relatively independent subunits because it is derived from different developmental tissues and performs a diversity of functions (Cheverud, 1995; Hallgrímsson et al., 2007; Willmore et al., 2006). A commonly addressed question is whether a general pattern of so called "modularity" exists in skulls across species of clade (e.g., Bardua et al., 2019; Raidan et al., 2021; Randau et al., 2019; Sanger et al., 2012). Others of explored the magnitude of within-module integration, showing that within a range of taxa different skull modules can vary a lot (e.g., Bardua et al., 2019; Raidan et al., 2021), but whether the magnitude of integration has an influence on the potential for phenotypic variation is unclear (e.g., Bardua et al., 2019; Felice et al., 2018; Goswami & Polly, 2010; Rhoda et al., 2021). The mammalian skull has become a seminal system in which to investigate the influences of modularity on evolutionary processes (e.g., Drake & Klingenberg, 2010; Goswami & Polly, 2010; Marroig et al., 2009). The mammalian face is thought to be more evolutionary labile (capable of

Received July 7, 2022; accepted February 6, 2023

evolutionary change) than the braincase because it appears to be more disparate across mammalian species (e.g., Bennett & Goswami, 2013; Marcus et al., 2000). However, the precise mechanisms behind disparity of skull modules remains elusive. Further research using diverse clades with differing evolutionary histories is needed to build a knowledge-base on the influence of modularity and integration on morphological disparity and macroevolutionary patterns of diversity.

Here, we demonstrate the utility of a multilevel study design to elucidate the influence of modularity upon patterns of evolutionary diversity using an overlooked taxonomic group to examine these questions: the Leporidae (rabbits and hares). They have a surprising amount of morphological, behavioral, and lineage diversity (Alves et al., 2008a; Kraatz et al., 2021). Their skull is notable because its shape is related to locomotor behavior, a rare functional relationship among mammals (Bramble, 1989; Kraatz & Sherratt, 2016; Kraatz et al., 2015). Fast running (i.e., cursorial) species show a more ventrally tilted face, pivoting at the anterior edge of the braincase; hopping species present dorsal arching, but they typically have a shallower tilt angle (Kraatz & Sherratt, 2016; Kraatz et al., 2015). Thus, changes in the leporid skull related to locomotor behavior appear to happen in specific skull regions, which may correspond to modules.

The biological hypothesis is morphological diversity in the leporid skull arises from the modular composition, either by different modular patterns among species, or different contributions of modules in a consistent modular pattern. We first evaluate three hypotheses of modularity proposed for the mammalian skull (Cheverud, 1995; Hallgrímsson et al., 2007; Willmore et al., 2006). Preliminary analysis showed the null hypothesis of no modular pattern was not supported. Finding one hypothesis supported at all levels, we investigate how those modules differ in terms of their morphological disparity and strength of integration and infer which module drives patterns of cranial variation across these levels. The contribution of allometry to patterns of covariation is also evaluated at each level. This is the first study to explicitly investigate skull modularity and integration among species of leporids, building upon knowledge provided by single species representatives in previous class-wide studies (Esteve-Altava, 2021; Marroig et al., 2009; Porto et al., 2009).

Methods

All analyses were performed using the R Statistical Environment v. 4.2.1 (R Development Core Team, 2022), using the *geomorph* package v.4.0.4 (Adams et al., 2022) unless otherwise stated, with statistical significance estimated using a permutation approach (1,000 iterations) and evaluated at the significance level of 5%.

Samples

We sampled 317 specimens from 22 species across Leporidae representing the main lineages (Supplementary Table S1), many of which featured in a previous study (Kraatz & Sherratt, 2016), using predominantly museum collections (details in Supplementary File 1). For *Oryctolagus cuniculus* and *Lepus europaeus*, we could increase sampling with whole carcasses scavenged from pest control activities in Australia (ethics approved, details given in Acknowledgments), where these species were introduced on multiple occasions during the 1800s by European settlers from UK stocks (Peacock & Abbott, 2013; Stott, 2015). As the most widely distributed of all leporids, we restricted the *O. cuniculus* (herein *Oryctolagus* for brevity) samples in this study to those from Europe and Australia to limit population-level variation.

Specimens were scanned by X-ray computed tomography (CT) to obtain digital models of the cranium for measurement. Scans of museum specimens were made using a J. Morita Veraviewepocs 3D R100 system (College of Dental Medicine, Western University of Health Sciences), typically operated at 75 kV and 3 mAs with voxel size ranging from 125 to 160 µm. Whole specimens of *Oryctolagus* and *L. europaeus* were scanned using a Siemens SOMATOM Force CT scanner (Dr Jones & Partners, The South Australian Health and Medical Research Institute [SAHMRI], Adelaide). The scanner was operated at 120 kVp and 200 mA, with one second exposure and a slice thickness of 0.4mm.

Scan acquisition and landmark placement

The CT tomograms were processed with Checkpoint (Stratovan Corporation, Davis, CA), thresholding by voxel gray value to obtain an isosurface representing bone. Then landmarks were manually digitized on the crania models by one author (BK); following Kraatz and Sherratt (2016), 44 landmarks were placed at homologous points on the cranium, over the left and right sides, and the curve tool was used to place eight equally spaced semilandmarks along the sagittal axis of the cranial roof to capture the arching curvature (Figure 1, Supplementary Table S2). Zygomatic arches were then digitized with the landmark tool using as many points necessary to capture the complex curves, and these landmarks were converted into 11 equally spaced semilandmarks each using the "digit.curves" R function. Missing landmarks, typically reflecting breaks in supraorbital process or regions of the basicranium, were an issue for 45 specimens (details in Figshare repository). The positions of these missing landmarks were estimated using a thin-plate spline approach (Gunz et al., 2009), where each missing landmark is predicted among all other homologous landmarks of complete specimens of the same species, implemented using the "estimate.missing" function.

The landmark coordinate data were aligned using a generalized Procrustes superimposition (Rohlf & Slice, 1990), taking into account object symmetry and allowing semilandmarks of the cranial roof and zygomatic arches to slide along their tangent directions in order to minimize bending energy (Gunz et al., 2005), implemented with "bilat.symmetry" function. The resulting symmetric component of shape (sensu Klingenberg et al., 2002) was used in the following analyses.

Hypotheses of modularity

Preliminary analysis rejected the hypothesis of no modular structure in the leporid cranium, so we proceeded with evaluating three alternative modular hypotheses proposed for mammalian skulls (Cheverud, 1995; Hallgrímsson et al., 2007; Willmore et al., 2006) (Table 1). The "tissue origin" hypothesis (Figure 1B) use two modules based upon whether bones originate from neural crest or mesoderm cells (Willmore et al., 2006). The "developmental groups" hypothesis (Figure 1C) identifies three modules based upon embryological development (Hallgrímsson et al., 2007), where the basicranium is derived from the chondrocranium, the neurocranium from dermatocranium bones of the cranial vault, and the face from the splanchnocranium initially with subsequent influence of dermatocranial elements. The "functional groups" hypothesis (Figure 1D) has four modules based upon different

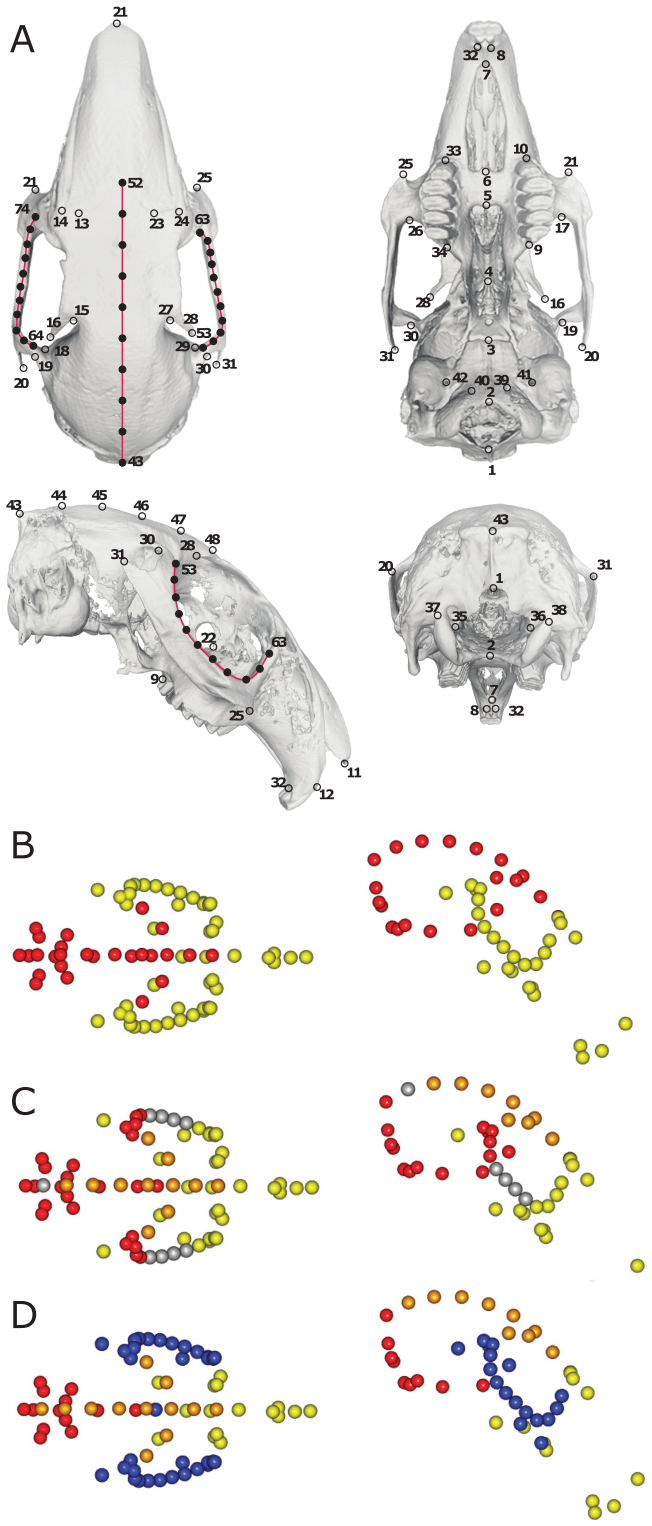

Figure 1. Cranium landmarks (A) and modular hypotheses, tissue origin (B), developmental groups (C), and functional groups (D). The three modularity hypotheses in Table 1 are depicted in dorsal (left) and lateral (right) views. Landmark numbers refer to Supplementary Table S2. Gray landmarks are not used in the modular hypothesis.

functional regions of the cranium (Cheverud, 1995; Willmore et al., 2006) and related to the six-module hypothesis found across many mammals (Cheverud, 1982a; Goswami, 2006). The six-module hypothesis was not investigated here due its similarity to the "functional groups" hypothesis and because the derived morphology of the elongated rostrum of leporids, which is divided dorso-ventrally in the six-module hypothesis, has been shown in previous studies (Kraatz & Sherratt, 2016) to be a key region that varies coherently within the leporid cranium.

Datasets

The Procrustes landmark data were divided into three datasets that represent different biological levels. The first level is within-species variation, and the monospecific *Oryctolagus* was used because it has the largest sample size (N = 60) and is an exemplary biological model, and often used to represent leporids as a whole. The second level is the within-genus level, where the hares (or jack-rabbits, *Lepus*) and cottontail rabbits (*Sylvilagus*), were used because they are the most speciose in Leporidae and both represent monophyletic clades. Here they are represented by six and seven species each (N = 97 and N = 110, respectively). We followed Cano-Sánchez et al. (2022) in their taxonomic recommendation that the pygmy rabbit *Sylvilagus idahoensis* (Merriam, 1891; previously *Brachylagus*) be included with the *Sylvilagus* radiation (e.g., Grinnell et al., 1930) because phylogenetic inference has consistently recovered this taxon as sister or nested within *Sylvilagus* (Cano-Sánchez et al., 2022; Matthee et al., 2004). To account for the group structure in each of these levels, an analysis of variance (ANOVA), implemented with "procD.lm" function, was used to evaluate the proportion of variance attributed to population for *Oryctolagus*, and species for *Sylvilagus* and *Lepus*. Residuals of these ANOVAs were extracted to represent the pooled-within group shape for subsequent analyses of integration and disparity.

The third level is the among-species "evolutionary" level, represented by species-averaged cranial shape data of 22 species across the family (e.g., Klingenberg & Marugan-Lobon, 2013). Other than *Lepus* and *Sylvilagus*, the family is represented by monotypic or low diversity genera. We used a published phylogenetic hypothesis based upon seven genes (five nuclear and two mitochondrial) (Matthee et al., 2004). The tree was pruned to 21 species included in this study using "drop.tip" function in *ape* v.5.6-2 (Paradis et al., 2004). *Lepus europaeus* was not included in Matthee et al.'s original analysis. Based upon other molecular analyses and the propensity for *L. europaeus* to hybridize (Alves et al., 2008b; Ashrafzadeh et al., 2018; Ben Slimen et al., 2008; Melo-Ferreira et al., 2012; Suchentrunk et al., 2008), we applied the analyses to two alternate topologies: *L. europaeus* sister to *L. capensis*, and sister to *L. timidus*. We grafted *L. europaeus* onto the tree using "bind.tip" function in *phytools* v.1.0-1 (Revell, 2012); preliminary analysis tested different branch lengths with inconsequential changes to results, so we positioned the node halfway along the original branch in both topologies (Supplementary Figure S2).

Statistical analyses

Principal components analysis was used to identify over how many axes the shape variance was distributed at each level, and thus gives an indication of the magnitude of integration for the whole cranium, where higher integration results in more variance contained in relatively few dimensions. This was implemented using the "gm.prcomp" function. Because integration is expected to be influenced by allometry, the covariation of shape and size, we investigated two types of allometry: static allometry, which is the relationship of shape

Table 1. Hypotheses of modularity.

Tissue origin (Willmore et al., 2006)	Developmental groups, (Hallgrímsson et al., 2007)	Functional groups, (Willmore et al., 2006)
Neural crest (48)	Face (30)	Face (16)
Mesoderm (26)	Neurocranium (11)	Temporal (33)
	Basicranium (24)	Cranial vault (12)
	Omitted (9)	Basicranium (13)

The number landmarks per module are given in parentheses. See Figure 1 for graphical representation. For developmental groups, nine semilandmarks were omitted as these fell along module boundaries.

and size among individuals of the same age class in a species/clade; and evolutionary allometry, which is the relationship of shape and size among species, and defined as the covariation of shape and size along branches of the phylogenetic tree. Multivariate regressions were used to assess the amount of shape variation of the whole cranium attributed to allometry (Monteiro, 1999) at each level. The regression score approach (Drake & Klingenberg, 2008) was used to visualize the allometric relationships with log-transformed centroid size, a measure of size derived from the landmark coordinates and calculated during Procrustes superimposition. The degree of static allometry was assessed in *Oryctolagus*, and *Sylvilagus* and *Lepus* genera by performing a regression on all specimens using "procD.lm". The regression model included species (or population for *Oryctolagus*), allowing the interaction of size and species to be evaluated. Evolutionary allometry was examined among species using a phylogenetic ANOVA (PGLS) (Adams, 2014b), with species mean values of shape and size, implemented with "procD.pgls." The residuals of the statistically significant models were extracted and used to represent shape with the allometric component removed ("allometry-free").

We tested the three a priori defined hypotheses of modularity and evaluated which was the most supported for the data, using the covariance ratio (CR) and post-hoc effect size approach (Adams & Collyer, 2016, 2019). The CR coefficient was calculated for each hypothesis using the "modularity.test" function. Effect sizes from each modularity analysis were evaluated using the "compare.CR" function to infer which of the modular hypotheses is most supported by the data. This test was performed using the pooled-within species residuals and allometry-free datasets of *Oryctolagus*, *Lepus*, and *Sylvilagus* genera. For the evolutionary level, we used the "phylo.modularity" function to calculate CR in a phylogenetic context, which used the evolutionary covariance matrix among traits found under a Brownian motion model of evolution (Adams & Felice, 2014).

Analyses of modularity and integration typically require large sample sizes (e.g., minimum of 30 specimens per species (Haber, 2011)), which can be problematic for macroevolutionary studies. To understand the uncertainty that sample size may give in our results, we used a subsampling approach taking 10 specimens at random from the *Oryctolagus* dataset, calculated the test for modularity (details above), and repeated this 100 times to obtain an estimate of the margin of error. We then calculated the CR of each hypothesis for all species with a sample size of at least 10 to provide preliminary insights into modular variation across the clade.

The consensus, best supported modular hypothesis at each level was used to investigate which module contributes the most to the observed variation among individuals, and how cranial modules vary in terms of morphological disparity and strength of within and between module integration. Each module was subjected to a separate GPA to avoid correlations between modules due to the superimposition (Cardini, 2019b), transformed to account for pooled-within group variation as above, and multiplied by module centroid size to ensure each module represents the original relative proportions (necessary for disparity). Since GPA influences the covariance structure among landmarks, whether to use a single or separate GPA is a matter of discussion in geometric morphometrics (Cardini, 2019b; Goswami et al., 2019; Klingenberg, 2021); our preliminary analysis showed a separate GPA changes the magnitude of results, but the overall among-module patterns are equivalent to a single GPA (Supplementary Figure S1). We used Mantel's test to compare a distance matrix of between-individual distances calculated from all landmarks to one calculated from landmarks within a module. This was implemented with the "mantel" function in *vegan* R package v.2.6-2 (Oksanen et al., 2022). The highest correlation value indicates that module contributes the most to the overall morphospace. To measure morphological disparity, we used the Procrustes variance (the sum of the diagonal elements of the covariance matrix (Zelditch et al., 2012)) divided by the number of landmarks in the module. This was implemented using the "morphol.disparity" function. Higher values represent greater variation in shape among observations (wider spread in morphospace). To measure the magnitude of integration *within* each module, we calculated the relative eigenvalue variance (Pavlicev et al., 2009) and from this the standardized effect score (Z-score) as per (Conaway & Adams, 2022) implemented with "integration.Vrel" function. This provides a directly comparable measure of the magnitude of integration across levels and modules, based upon the degree of eigenvalue dispersion, that is how variance is distributed across eigenvalues. Higher negative values of the effect score represent lower covariance between shape traits, which means weaker integration. The effect sizes were compared for significant differences using the "compare.ZVrel" function. Finally to measure the magnitude of integration *between* modules at each level, two-block partial least squares analysis (PLS) was used (Adams & Felice, 2014; Rohlf & Corti, 2000), implemented with functions "two.b.pls" and "phylo.integration". This approach calculates the correlation coefficient (r-PLS) between two matrices ("blocks") of traits, where values closer to 1 mean stronger integration between modules.

To understand how much phylogenetic relatedness is driving morphological variation, phylogenetic signal was evaluated for the whole skull and per module using the K_{mult} approach (Adams, 2014a). The metric, based upon K

(Blomberg et al., 2003), measures the proportion of the tip variance that is explained by a Brownian motion (BM) process for the tree, thus testing whether relatives resemble each other less than expected under BM (K less than 1), which suggests a departure from Brownian motion evolution and indicates homoplasy. Where there is a K value greater than one, close relatives are more similar than expected under BM (strong phylogenetic structure). This was implemented with "physignal" function.

Results

Within-species: Oryctolagus

Principal components analysis (PCA) of *Oryctolagus* produced five PC axes each contributing more than 5% of the total variance (PC1–5 = 53.8%). Multivariate regression revealed 13.2% ($p < .001$) of the shape variation is attributed to static allometry and 9.8% to population differences. There was no significant interaction, indicating similar allometric slopes between populations (Figure 2A).

Testing for modularity in the cranium using the covariance ratio (CR) approach, both Procrustes coordinates and regression residuals (allometric variation removed) gave similar patterns among the four module hypotheses; comparing effect sizes showed functional groups hypothesis to have the highest effect size, although it was not significantly different to the other hypotheses (Table 2, Figure 3A). Subsample analysis of *Oryctolagus* found "functional groups" to be supported 84% of the time, "developmental groups" 6% and "tissue origin" 10%. After allometry was removed, this changed to 83%, 8%, and 10%, respectively.

Examining each module of the "functional groups" hypothesis revealed the face module produced the most similar pattern among-specimen variation to that of whole cranium shape, as revealed by Mantel's test (Figure 4A). The face module exhibited the greatest morphological disparity, while the cranial vault had the lowest (Figure 4B). The temporal modules had the highest effect size of relative eigenvalue variance (low integration), while the cranial vault and face showed the lowest (high integration) (Figure 4C). However, there were no significant pairwise differences in the relative eigenvalue variance based upon their effect sizes. Removing allometric variation did not have any appreciable effect on the results (Figure 4).

Within-genus level: Sylvilagus

Using pooled-within species residuals, PCA of *Sylvilagus* produced two PC axes each contributing more than 5% of the total variance (PC1–2 = 65.8%). Multivariate regression revealed 46.8% of the shape variation is attributed to

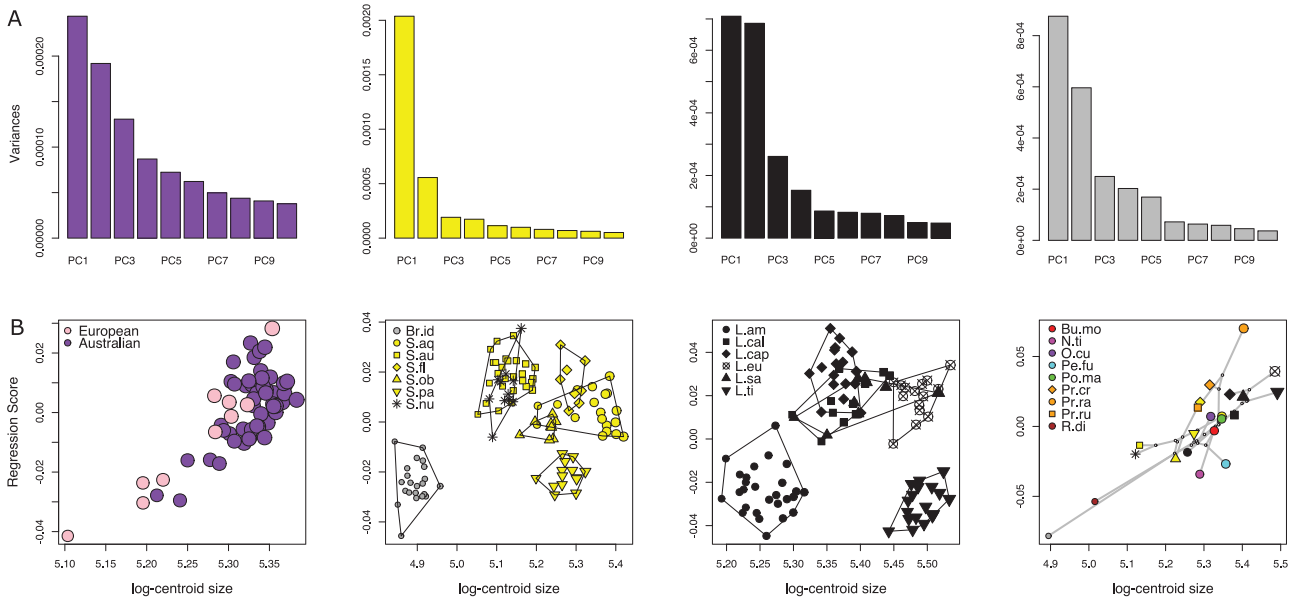

Figure 2. (A) Whole cranium integration as given by screeplots of eigenvalues of the principal component analysis at each level. (B) Whole cranium multivariate regressions showing allometric component of shape at each level.

Table 2. Results of the covariance ratio (CR) test for within-species modularity (60 specimens of *Oryctolagus*).

Modularity hypothesis	All shape variation		Allometry-free shape	
	CR	Effect size	CR	Effect size
Tissue origin	0.837 (0.0379)	−3.632 (1.463)	0.818 (0.0406)	−3.511 (1.414)
Developmental groups	0.784 (0.0334)	−3.316 (0.911)	0.746 (0.0386)	−3.337 (0.907)
Functional groups	0.718 (0.0327)	**−4.158 (0.965)**	0.692 (0.0351)	**−3.971 (0.914)**

Tests were performed on the pooled within-population residuals "all shape variation," and the regression residuals "allometry-free variation". All tests were significant at the $\alpha = 0.05$ level (p-values not shown). Standard deviations (given in parentheses) are based upon 100 iterations of a subsample of 10 specimens. Most supported hypothesis in bold. Effect size significance based upon 1000 permutations.

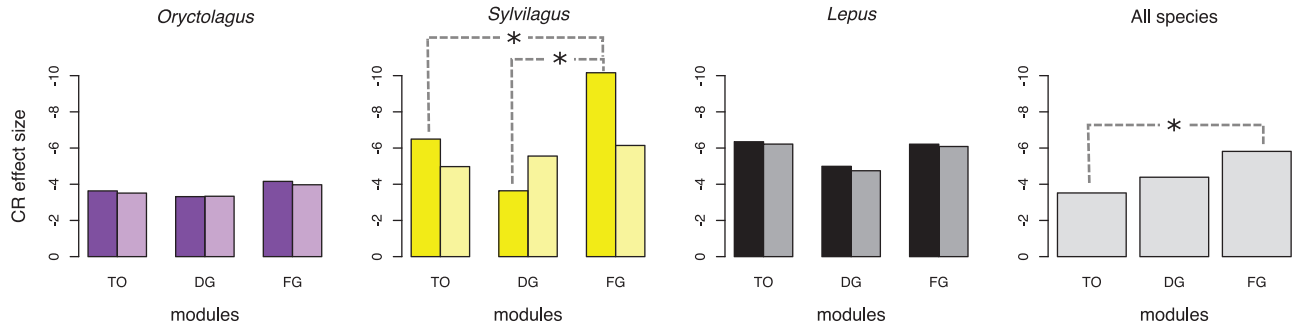

Figure 3. Evaluating modular hypotheses with the covariance ratio (CR). The effect size is plotted for each modular hypothesis: tissue origin (TO), developmental groups (DG), and functional groups (FG). Tests were performed on the Procrustes shape variables (solid, all shape variation), and the regression residuals (lighter shade, allometry-free variation). Evolutionary level (all species is with allometry only). Pairwise significant results ($\alpha = 0.05$) are shown with asterisks.

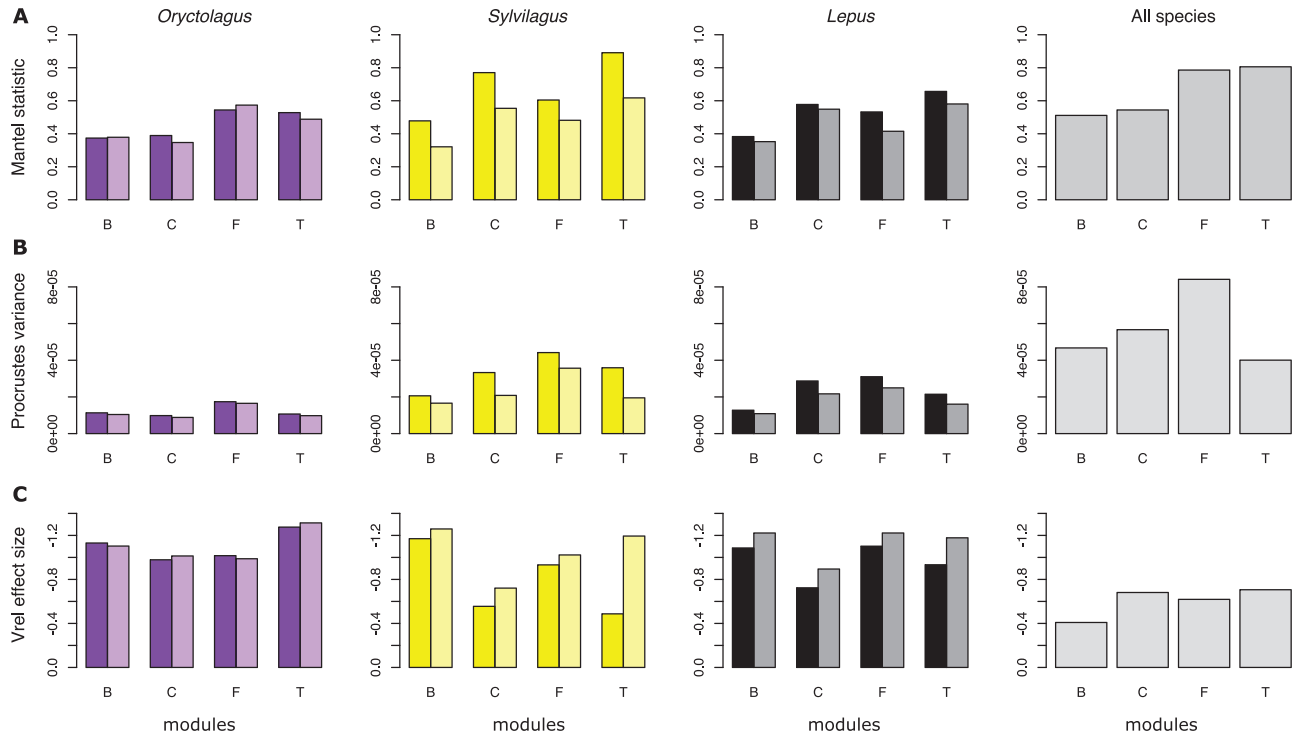

Figure 4. Results of three tests performed on each module of the "functional groups" hypothesis across all levels. Modules: B = basicranium, C = cranial vault, F = face, T = temporal. (A) Mantel tests for similarity with whole cranium patterns of among-specimen variation. (B) Morphological disparity as given by the Procrustes variance. (C) Morphological integration within modules as given by effect size (Z-score) of relative eigenvalue variance (Vrel). Tests were performed on the Procrustes shape variables (solid, all shape variation), and the regression residuals (transparent, allometry-free variation). Evolutionary level (all species is with allometry only). Columns represent levels: within-species level comprising *Oryctolagus* ($N = 60$); within-genus levels across *Sylvilagus* and *Lepus*; among species level from 22 species across family (based upon *europaeus-capensis* sister pair).

allometry, 4.2% accounts for species variation and a significant interaction term reveals 1.4% is due to one or more species-specific allometric slopes (Figure 2B).

Among the *Sylvilagus* species was consensus support for the "functional groups" hypothesis using the CR approach (Supplementary Table S3), and from a pooled-within species analysis the "functional groups" hypothesis was significantly better than other hypotheses (Figure 3B). Removing allometry lowered all effect sizes to be not significantly different from each other but the "functional groups" hypothesis remained with the highest effect size.

The temporal module showed the most similar patterns of among-specimen variation to that of whole cranium shape (Figure 4B). The face module exhibited the greatest disparity, while the basicranium had the lowest (Figure 4B). The basicranium module showed the highest effect size of relative eigenvalue variance (low integration), while the temporal module had the lowest (high integration) (Figure 4C). Significant pairwise differences in the relative eigenvalue variance based upon their effect sizes were found between the basicranium and all other modules, and between the cranial vault and face. Removing allometric variation had a great influence the integration tests so that the cranial vault became the highest integrated (Figure 4C).

Within-genus level: Lepus

Using pooled-within species residuals, PCA of *Lepus* produced four PC axes each contributing more than 5% of the total

Table 3. Phylogenetic signal of whole cranium shape, and each of the four modules of the "functional groups" hypothesis (22 species), using topology where *Lepus europaeus* is sister to *L. capensis* (see Supplementary Table S4 for alternative).

	K_{mult}	Effect size	*p* value
Whole cranium	0.704	1.5539	.074
Basicranium	0.672	1.1129	.139
Cranial vault	0.720	1.6106	.06
Face	0.779	1.7807	.043
Temporal	0.641	1.0391	.16

Effect size significance based upon 1000 permutations.

Table 4. Results of the phylogenetic covariance ratio (CR) test for family-level modularity (species), using topology where *Lepus europaeus* is sister to *L. capensis* (see Supplementary Table S5 for alternative).

Modularity hypothesis	All shape variation	
	CR	Effect size
Tissue origin	**0.944**	**–3.519**
Developmental groups	0.913	–4.388
Functional groups	0.875	–5.815

All tests were significant at the α = 0.05 level (*p*-values not shown). Most supported hypothesis in bold. Effect size significance based upon 1000 permutations.

variance (PC1–4 = 64.4%). Multivariate regression revealed 18.5% of the shape variation is attributed to allometry, 7.6% accounts for species variation and a significant interaction term reveals 8.9% is due to one or more species-specific allometric slopes. The first and second PC axes contribute similar amounts to the total variance (PC1 = 25.2%, PC2 = 24.4%).

Among the *Lepus* species the "functional groups" hypothesis was supported in all but one species using the CR approach (Supplementary Table S3), and from a pooled-within species analysis the "tissue origin" and "functional groups" hypothesis had equally greater effect sizes over "developmental groups", but no pairwise comparison was significant (Figure 3C). Removing allometry lowered all effect sizes but did not change the pattern.

Based on the consensus (Supplementary Table S3) the "functional groups" hypothesis was investigated further. The temporal module showed the most similar patterns of among-specimen variation to that of whole cranium shape (Figure 4A). The face module exhibited the greatest disparity, while the basicranium had the lowest (Figure 4B). The face and basicranium modules had the highest effect size of relative eigenvalue variance (low integration), while the cranial vault had the lowest (high integration) (Figure 4C). However, there were no significant pairwise differences in the relative eigenvalue variance based upon their effect sizes. Removing allometric variation did not have any appreciable effect on the results.

Among-species level: Leporidae family

PCA of 22 species produced 5 PC axes each contributing more than 5% of the total variance (PC1–5 = 84.3%) with both tree topologies. A phylogenetically informed multivariate regression of species averages was not statistically significant but indicated 6.9% (*p* = .287) of the shape variation is attributed to size variation if *L. europaeus* is sister to *L. capensis*, or 11.3% (*p* = .204) if *L. europaeus* is sister to *L. timidus* (Figure 2D). Thus, proceeding analyses were done without correcting for allometry.

There is no significant phylogenetic signal in the whole cranium or in any module (Table 3, Supplementary Table S4), except a marginally significant value for face module when *L. europaeus* – *L. capensis* are considered as sister species (Table 3). All K_{mult} estimates are well below 1, indicating there is much less phylogenetic signal than expected under a Brownian motion model of evolution (i.e., homoplasy).

Among all species with a sufficient sample size to estimate CR, the "functional groups" hypothesis was largely supported (Supplementary Table S3). With a phylogenetic CR analysis of average shapes for 22 species, the functional groups hypothesis had the best support and was significantly greater than the "tissue origins" hypothesis (Figure 3, Table 4, Supplementary Table S5). Both topologies produced the same patterns. The facial and temporal modules showed the most similar patterns of among-species variation to that of whole cranium shape (Figure 4A). The face module exhibited the greatest disparity, while the temporal had the lowest (Figure 4B). The temporal and cranial vault module had the highest effect size of relative eigenvalue variance (low integration), while the basicranium had the lowest (high integration) (Figure 4C). However, there were no significant pairwise differences in the relative eigenvalue variance based upon their effect sizes.

Discussion

This study aimed to investigate whether patterns of integration and modularity in the leporid cranium are consistent across three biological levels of variation: within a species, within genera (using two speciose radiations), and among 22 species of the Leporidae family. Our results present a mixture of consistency and variability. We found that the way the cranium is partitioned into modules is consistent, and the same module displays greatest disparity across levels. Removing the allometric component of shape also had a uniform effect of reducing the magnitude of disparity and integration, generally without changing overall patterns. However, other aspects differed across levels: how much allometry contributes to variation, patterns of whole skull integration, which module contributes the most to overall morphospace, and patterns of within-module integration all show variability among the datasets. These results indicate the complexity of biological diversity, and the scalable hierarchy hypothesis is mostly rejected in this study system. The implications of these results are discussed below.

A modular mammalian skull with prominent facial disparity

Boundaries of cranium modules may vary among closely related species of a clade or radiation (e.g., Parsons et al., 2018; Raidan et al., 2021; Randau et al., 2019; Sanger et al., 2012) or be remarkably conserved over vast evolutionary distances (e.g., Marshall et al., 2019; Singh et al., 2011). Many studies of mammal crania have found support for a hypothesized six-module structure (e.g., Cheverud, 1995; Goswami & Polly, 2010; Randau et al., 2019; Heck et al., 2018). Our multilevel analyses concur with this finding; although we tested the simpler four module "functional groups" hypothesis (e.g., Willmore et al., 2006), all levels showed greatest support for this pattern of modularity. This lends support to hypothesis that overall diversity in the mammal skull is likely driven by evolutionary processes invoking changes in some modules independently of others..

Akin to the pattern observed across mammals (e.g., Marcus et al., 2000; Usui & Tokita, 2018), this study shows prominent facial disparity at all levels. The face and temporal modules together contributed the most to the variation among all 22 leporid species, which echoes the principal axis of diversity in a previous study (Kraatz & Sherratt, 2016). Domestication of rabbits appears to have profited from this and taken diversity of the facial region to greater levels than their wild counterparts (Geiger et al., 2022). Variation in the facial region among individuals of a species may be related to phenotypic plasticity invoked by mastication and diet (e.g., Menegaz et al., 2009; Pucciarelli et al., 1990) but is also associated with genetic variance (e.g., Atchley et al., 1981; Mossey, 1999). While among species variation in the facial region can be attributed to natural selection as well as a property of allometry; it has been suggested that face length variation is a ubiquitous outcome of body size evolution (Cardini, 2019a; Cardini & Polly, 2013). In leporids, variation in the facial region, specifically the angle of facial tilt, has been shown to relate to their locomotive ability (Kraatz & Sherratt, 2016; Kraatz et al., 2015). We propose that like other systems (e.g., Evans et al., 2017; Machado et al., 2018; Neaux et al., 2018; Sanger et al., 2012) it is through the modular composition of the skull that the evolutionary potential of the face has been realized.

A scalable hierarchy of diversity

Multilevel analyses are a valuable tool to test whether the processes responsible for variation within a species may facilitate adaptive variation among species (Benítez et al., 2022; Klingenberg, 2014; Monteiro & Nogueira, 2010; Monteiro et al., 2005; Urošević et al., 2018; Young & Badyaev, 2006). Theoretically, consistent patterns of integration should result from consistent selection pressures operating during trait development or function (Cheverud, 1982a, 1995; Lande, 1980), which leads to the scalable hierarchy hypothesis. However the reality is there is no consensus in the literature; some clades have shown historical persistence of patterns across levels (e.g., Benítez et al., 2022; Young & Badyaev, 2006) while others find shifts in integration patterns at different levels, which may be due to selection for different functional demands (e.g., Monteiro et al., 2005; Randau et al., 2019; Urošević et al., 2018).

Our study shows each level comprises a mix of consistent and unique patterns of variation. The modular composition is retained between static and evolutionary levels, but patterns of whole skull integration vary, as does module-by-module disparity and integration patterns. These results suggest that different processes are responsible for trait covariation (Klingenberg, 2014). The challenge for future researchers will be to tease apart the effects of functional, developmental, genetic, and environmental integration patterns, which requires multilevel analyses and broader scale taxonomic sampling.

Can modularity facilitate evolutionary diversity?

Taking the multilevel approach a step further, we contrasted two speciose radiations to provide insights into how evolutionary processes acting on a modular system can result in divergent diversification patterns. The hares (or "jack-rabbits") of the *Lepus* genus are generally cursorial specialists and the New-World rabbits (*Sylvilagus*) are mostly generalists with a hopping gait. While we find that variation in the cranium among both genera is mostly due to the cranial vault and temporal modules (Figure 4A), the way in which each clade varies these two modules results in very different axes of diversity (Figure 5). These clades have notable differences in the degree of facial tilt (Kraatz & Sherratt, 2016); *Lepus* have mostly strongly downward-tilted rostra to facilitate visual acuity during speed, but there is wide variation in this trait among species. *Sylvilagus* on the other hand present a shallower tilt and less variation among species. Thus, different selection pressures resulting from their behavioral differences influence the same modules but each module responds differently, resulting in evolution along diverging trajectories in morphospace. To achieve facial tilt involves coordinated changes in the cranial vault and temporal modules alongside the other modules, but we posit that the modular composition has facilitated the greater diversity of morphologies to evolve, as exemplified by the *Lepus* and *Sylvilagus* radiations.

Whether the magnitude of integration in a structure has an influence on the potential for phenotypic variation is unclear (e.g., Bardua et al., 2019; Felice et al., 2018; Goswami and Polly, 2010; Rhoda et al., 2021). Our results do not show a consistent relationship between the strength of within-module integration and how much morphological disparity is present in the module (Figure 4). Several other studies on diverse taxa have found the same relationship (Bardua et al., 2019, 2020; Randau et al., 2019; Watanabe et al., 2019). In a study at the evolutionary level, Linde-Medina et al. (2016) suggested that the face module has greater capacity to respond to selection as compared with the braincase, and thus the greater disparity of the face module may more likely be due to faster morphological evolution in this module. These results adhere to the expectations outlined by Goswami et al. (2014) and Felice et al. (2018) that the relationship between the magnitude of integration and morphological disparity is mediated by the rate of evolution, and integration will only drive disparity when the direction of selection aligns with the trajectory of trait covariation.

Allometry and the effects of size

Body size is a dominant factor influencing how structures are morphologically integrated (Gould, 1966; Marroig & Cheverud, 2005, 2010; Nijhout, 2011). Therefore, considering separately form (shape with size), allometry-included shape, and allometry-free shape is necessary when evaluating patterns of trait covariation. We found that the strength of integration to be lower in allometry-free analyses (e.g., Porto et al., 2013; Randau et al., 2019; Urošević et al., 2018),

which is to be expected as some variance is being removed. However, like Randau et al. (2019) and Urošević et al. (2018), but unlike Porto et al. (2013), our allometry-free results presented largely the same pattern as those derived from all data. This difference probably lies in the methodological differences to quantifying trait variation (i.e., landmarks vs. inter-landmark distances, see Machado et al., 2019 for a review) and the treatment of size (scale); the scaling step of the Procrustes superimposition, which removes isometric variation, results in shape data, while inter-landmark distances inherently retain size data and present form. Thus in all studies, allometry was removed but the starting point was different (shape in ours, Randau et al. (2019) and Urošević et al. (2018) versus form in Porto et al. (2013)).

Including a multilevel analysis of allometry in this study provided an opportunity to address the standing question of whether there are consistent patterns among static and evolutionary allometry (e.g., Cheverud, 1982b; Klingenberg & Zimmermann, 1992; Pelabon et al., 2014), the classic example of biological hierarchy. We found the three of the four datasets to be consistent in how much shape was predicted by size: the evolutionary level, within species and within one genus (*Lepus*) all had less than 20%, while *Sylvilagus* genus had more than 40% attributed to allometry. This latter result was due in part to the very small body size of the Pygmy Rabbit (*S. idahoensis*), the smallest leporid species. Only the static allometry levels were statistically significant. We posit that evolutionary allometry was not significant because the two speciose genera have diverging allometric trajectories. Visual inspection of the cranial shape change associated with allometry (Supplementary Figure S3) also highlights different patterns among levels; *Sylvilagus* presents the typical mammalian pattern of elongating the face and flattening the cranial vault with increasing size, while *Lepus* presents changes to the angle of the rostrum and zygomatic arches, features of facial tilt. These results indicate that evolutionary allometry in leporids is not an allometric "line of least evolutionary resistance" (sensu Marroig & Cheverud, 2005) derived from conserved static allometries. We predict that Leporidae will present ecologically driven diversity in their static (and

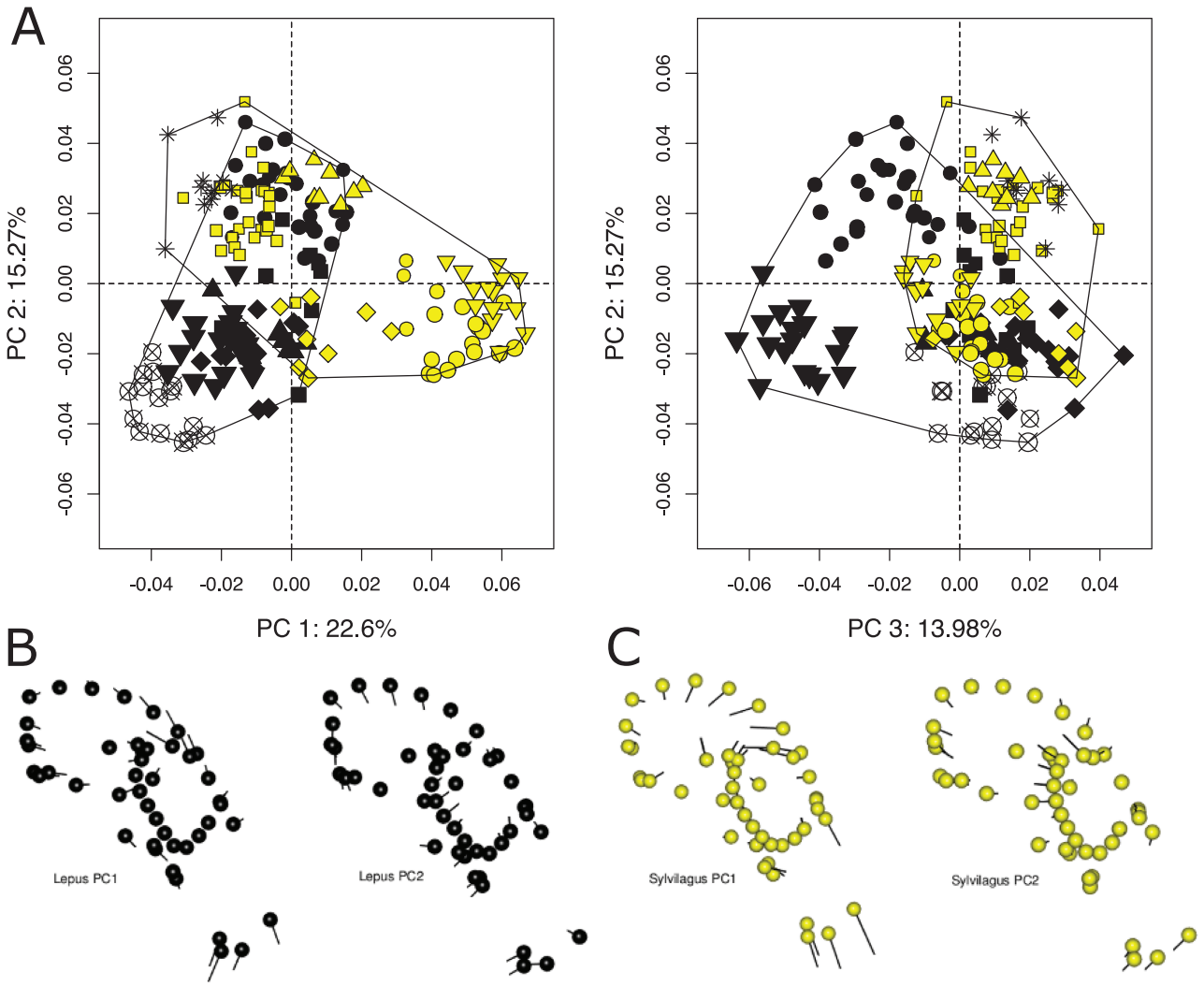

Figure 5. Morphospace of two generic-level radiations, *Sylvilagus* and *Lepus*, defined by the first three axes of a principal components analysis of Procrustes shape variables (without pooling by species, or removing allometric shape variation) (A). Convex hulls delimit each clade. Plotted points are scaled by cranium centroid size, and color and symbols as in Figures 3 and 4. Vector shape graphs depict the shape at the minimum PC score (dots) to shape at the maximum PC score (end of lines) along the first two PC axes from separate PCA of *Lepus* (B), and *Sylvilagus* clades (C), and highlight the differences in the two radiations' main dimensions of diversity and axes of allometric shape variation.

ontogenetic) allometries as seen in rodents (Dubied et al., 2021; Wilson, 2013; Zelditch & Swiderski, 2022) and this avenue of research is encouraged.

Conclusion

This study characterizes patterns of concordance in integration and modularity across hierarchical levels of evolution. In our study system, a conserved modular structure is evident across all levels. From that modular structure, evolutionarily processes acting on differences in module variation results in interspecific diversity. For example, comparing two generic-level radiations shows that unique selection pressures (e.g., locomotive strategies) are likely causing each module to evolve differently in morphospace. We also find that differences in module disparity and integration across levels refute the hypothesis that among-species variation is simply scaled up within-species variation. Therefore, in order to understand the complexity and uniqueness of biological variation at any level, a multilevel analysis is essential. This study shows the importance of targeting diverse clades beyond exemplars that are mostly frequently used to represent the overall diversity of life.

Supplementary material

Supplementary material is available online at *Evolution* (https://academic.oup.com/evolut/qpad020)

Data availability

Landmark data, specimen information, and code for analyses are provided on Dryad (https://doi.org/10.5061/dryad.4mw6m90f3). CT Scans are deposited to the MorphoSource repository (Project ID: 000415700).

Author contributions

Both authors designed the study and collected the CT scan data, B.K. collected the landmark data, E.S. analyzed the data, both authors interpreted the results and wrote the manuscript.

Conflict of interest: The authors declare no conflict of interest.

Acknowledgments

We thank the help of all the curators who provided access to specimens and facilities: Neil Duncan & Eileen Westwig (American Museum of Natural History), Jim Dines (Natural History Museum of Los Angeles County), Chris Conroy (Museum of Vertebrate Zoology, University of California, Berkeley), Judy Chupasko (Museum of Comparative Zoology, Harvard), Esther Lanang & Darrin Lunde (Smithsonian National Museum of Natural History), Shin-Ichiro Kawada (National Museum of Nature and Science, Tokyo), Christiane Funk (Museum für Naturkunde, Berlin), and David Stemmer (South Australian Museum), Thanks to Mishelle Korlaet at Dr Jones & Partners (Adelaide) for CT scanning support. Australian specimens donated by Peter Elsworth, DAF, BQ Toowoomba QLD (collected under ethics permit: CA2019/06/1288) and Pat Taggart, NSW DPI Orange NSW (collected under ethics permit: ORA 19/22/020). We also thank Faysal Bibi (Museum für Naturkunde) Anna Hardin (Western University of Health Sciences), Miriam Zelditch (University of Michigan), Gabriel Marroig (Universidade de São Paulo), P. David Polly (Indiana University) and two anonymous reviewers for comments that greatly improved the manuscript. Western University of Health Sciences funded B.K., and E.S. was supported by an Australian Research Council Future Fellowship (FT190100803) and a University of Adelaide Vice Chancellors' Research Fellowship.

References

Adams, D. C. (2014a). A generalized K statistic for estimating phylogenetic signal from shape and other high-dimensional multivariate data. *Systematic Biology*, 63(5), 685–697. https://doi.org/10.1093/sysbio/syu030

Adams, D. C. (2014b). A method for assessing phylogenetic least squares models for shape and other high-dimensional multivariate data. *Evolution*, 68(9), 2675–2688. https://doi.org/10.1111/evo.12463

Adams, D. C., & Collyer, M. L. (2016). On the comparison of the strength of morphological integration across morphometric datasets. *Evolution*, 70(11), 2623–2631. https://doi.org/10.1111/evo.13045

Adams, D. C., & Collyer, M. L. (2019). Comparing the strength of modular signal, and evaluating alternative modular hypotheses, using covariance ratio effect sizes with morphometric data. *Evolution*, 73(12), 2352–2367. https://doi.org/10.1111/evo.13867

Adams, D. C., Collyer, M. L., Kaliontzopoulou, A., & Baken, E. K. (2022). *geomorph: Software for geometric morphometric analyses*. R package version 4.0. https://CRAN.R-project.org/package=geomorph

Adams, D. C., & Felice, R. (2014). Assessing phylogenetic morphological integration and trait covariation in morphometric data using evolutionary covariance matrices. *PLoS One*, 9, e94335.

Alves, P. C., Ferrand, N., & Hackländer, K. (2008a). *Lagomorph Biology*. Springer Berlin, Heidelberg.

Alves, P. C., Melo-Ferreira, J., Freitas, H., & Boursot, P. (2008b). The ubiquitous mountain hare mitochondria: Multiple introgressive hybridization in hares, genus *Lepus*. *Philosophical Transactions Royal Society B*, 363(1505), 2831–2839. https://doi.org/10.1098/rstb.2008.0053

Ashrafzadeh, M. R., Djan, M., Szendrei, L., Paulauskas, A., Scandura, M., Bagi, Z., Ilie, D. E., Kerdikoshvili, N., Marek, P., Soos, N., & Kusza, S. (2018). Large-scale mitochondrial DNA analysis reveals new light on the phylogeography of Central and Eastern-European Brown hare (*Lepus europaeus* Pallas, 1778). *PLoS One*, 13, e0204653. https://doi.org/10.1371/journal.pone.0204653

Atchley, W. R., Rutledge, J. J., & Cowley, D. E. (1981). Genetic components of size and Shape. II. Multivariate covariance patterns in the rat and mouse skull. *Evolution*, 35(6), 1037–1055. https://doi.org/10.1111/j.1558-5646.1981.tb04973.x

Bardua, C., Fabre, A. C., Bon, M., Das, K., Stanley, E. L., Blackburn, D. C., & Goswami, A. (2020). Evolutionary integration of the frog cranium. *Evolution*, 74(6), 1200–1215. https://doi.org/10.1111/evo.13984

Bardua, C., Wilkinson, M., Gower, D. J., Sherratt, E., & Goswami, A. (2019). Morphological evolution and modularity of the caecilian skull. *BMC Evolutionary Biology*, 19(1), 30. https://doi.org/10.1186/s12862-018-1342-7

Ben Slimen, H., Suchentrunk, F., Stamatis, C., Marnuris, Z., Sert, H., Alves, P. C., Kryger, U., Shahin, A. B., & Elgaaied, A. B. A. (2008). Population genetics of cape and brown hares (*Lepus capensis* and *L europaeus*): A test of Petter's hypothesis of conspecificity. *Biochemical Systematics and Ecology*, 36, 22–39.

Benítez, H. A., Püschel, T. A., & Suazo, M. J. (2022). Drosophila wing integration and modularity: A multi-level approach to understand the history of morphological structures. *Biology,* 11, 567.

Bennett, C. V., & Goswami, A. (2013). Statistical support for the hypothesis of developmental constraint in marsupial skull evolution. *BMC Biology*, 11(52), 52.

Blomberg, S. P., Garland, T., & Ives, A. R. (2003). Testing for phylogenetic signal in comparative data: Behavioral traits are more labile. *Evolution*, 57(4), 717–745. https://doi.org/10.1111/j.0014-3820.2003.tb00285.x

Bramble, D. M. (1989). Cranial specialization and locomotor habit in the Lagomorpha. *American Zoologist*, 29(1), 303–317. https://doi.org/10.1093/icb/29.1.303

Cano-Sánchez, E., Rodríguez-Gómez, F., Ruedas, L. A., Oyama, K., León-Paniagua, L., Mastretta-Yanes, A., & Velazquez, A. (2022). Using ultraconserved elements to unravel Lagomorph phylogenetic relationships. *Journal of Mammalian Evolution*, 29(2), 395–411. https://doi.org/10.1007/s10914-021-09595-0

Cardini, A. (2019a). Craniofacial allometry is a rule in evolutionary radiations of placentals. *Evolutionary Biology*, 46, 239–248.

Cardini, A. (2019b). Integration and modularity in procrustes shape data: Is there a risk of spurious results? *Evolutionary Biology*, 46, 90–105.

Cardini, A., & Polly, P. D. (2013). Larger mammals have longer faces because of size-related constraints on skull form. *Nature Communications*, 4, 2458.

Cheverud, J. M. (1982a). Phenotypic, genetic, and environmental morphological integration in the cranium. *Evolution*, 36(3), 499–516. https://doi.org/10.1111/j.1558-5646.1982.tb05070.x

Cheverud, J. M. (1982b). Relationships among ontogenetic, static, and evolutionary allometry. *American Journal of Physical Anthropology*, 59(2), 139–149. https://doi.org/10.1002/ajpa.1330590204

Cheverud, J. M. (1995). Morphological integration in the saddle-back tamarin (*Saguinus fuscicollis*) cranium. *American Naturalist*, 145(1), 63–89. https://doi.org/10.1086/285728

Cock, A. G. (1966). Genetical aspects of metrical growth and form in animals. *Quarterly Review of Biology*, 41(2), 131–190. https://doi.org/10.1086/404940

Conaway, M. A., & Adams, D. C. (2022). An effect size for comparing the strength of morphological integration across studies. *Evolution,* 76, 2244–2259.

Drake, A. G., & Klingenberg, C. P. (2008). The pace of morphological change: Historical transformation of skull shape in St Bernard dogs. *Proceedings of the Royal Society of London. Series B*, 275, 71–76.

Drake, A. G., & Klingenberg, C. P. (2010). Large-scale diversification of skull shape in domestic dogs: disparity and modularity. *American Naturalist*, 175(3), 289–301. https://doi.org/10.1086/650372

Dubied, M., Montuire, S., & Navarro, N. (2021). Commonalities and evolutionary divergences of mandible shape ontogenies in rodents. *Journal of Evolutionary Biology*, 34(10), 1637–1652. https://doi.org/10.1111/jeb.13920

Erwin, D. H. (2000). Macroevolution is more than repeated rounds of microevolution. *Evolution and Development*, 2(2), 78–84. https://doi.org/10.1046/j.1525-142x.2000.00045.x

Esteve-Altava, B. (2021). Cranial anatomical integration and disparity among bones discriminate between primates and non-primate mammals. *Evolutionary Biology*, 49, 37–45.

Evans, K. M., Waltz, B. T., Tagliacollo, V. A., Sidlauskas, B. L., & Albert, J. S. (2017). Fluctuations in evolutionary integration allow for big brains and disparate faces. *Scientific Reports*, 7, 40431. https://doi.org/10.1038/srep40431

Felice, R. N., Randau, M., & Goswami, A. (2018). A fly in a tube: Macroevolutionary expectations for integrated phenotypes. *Evolution*, 72(12), 2580–2594. https://doi.org/10.1111/evo.13608

Geiger, M., Sánchez-Villagra, M. R., & Sherratt, E. (2022). Cranial shape variation in domestication: A pilot study on the case of rabbits. *Journal of Experimental Zoology. Part B. Molecular and Developmental Evolution*, 338(8), 532–541. https://doi.org/10.1002/jez.b.23171

Goswami, A. (2006). Cranial modularity shifts during mammalian evolution. *American Naturalist*, 168(2), 270–280. https://doi.org/10.1086/505758

Goswami, A., & Polly, P. D. (2010). The influence of modularity on cranial morphological disparity in Carnivora and Primates (Mammalia). *PLoS One*, 5(3), e9517. https://doi.org/10.1371/journal.pone.0009517

Goswami, A., Smaers, J. B., Soligo, C., & Polly, P. D. (2014). The macroevolutionary consequences of phenotypic integration: From development to deep time. *Philosophical Transactions of the Royal Society B*, 369(1649), 20130254. https://doi.org/10.1098/rstb.2013.0254

Goswami, A., Watanabe, A., Felice, R. N., Bardua, C., Fabre, A. -C., & Polly, P. D. (2019). High-density Morphometric analysis of shape and integration: The good, the bad, and the not-really-a-problem. *Integrative and Comparative Biology*, 59(3), 669–683. https://doi.org/10.1093/icb/icz120

Gould, S. J. (1966). Allometry and size in ontogeny and phylogeny. *Biological Review*, 41(4), 587–638. https://doi.org/10.1111/j.1469-185x.1966.tb01624.x

Grinnell, J., Dixon, J. S., & Linsdale, J. M. (1930). *Vertebrate natural history of a section of northern California through the Lassen Peak region*. University of California Press.

Gunz, P., Mitterocker, P., & Bookstein, F. L. (2005). Semilandmarks in three dimensions. In D. E. Slice (Ed.), *Modern Morphometrics in physical anthropology* (pp. 73–98). Kluwer Academic/Plenum Publishers.

Gunz, P., Mitteroecker, P., Neubauer, S., Weber, G. W., & Bookstein, F. L. (2009). Principles for the virtual reconstruction of hominin crania. *Journal of Human Evolution*, 57(1), 48–62. https://doi.org/10.1016/j.jhevol.2009.04.004

Haber, A. (2011). A comparative analysis of integration indices. *Evolutionary Biology*, 38(4), 476–488. https://doi.org/10.1007/s11692-011-9137-4

Hallgrímsson, B., Jirik, F. R., Lieberman, D. E., Liu, W., & Ford-Hutchinson, A. F. (2007). Epigenetic interactions and the structure of phenotypic variation in the cranium. *Evolution and Development*, 9(76), 91. https://doi.org/10.1111/j.1525-142X.2006.00139.x

Hansen, T. F., & Martins, E. P. (1996). Translating between microevolutionary process and macroevolutionary patterns: The correlation structure of interspecific data. *Evolution*, 50(4), 1404–1417. https://doi.org/10.1111/j.1558-5646.1996.tb03914.x

Heck, L., Wilson, L. A. B., Evin, A., Stange, M., & Sánchez-Villagra, M. R. (2018). Shape variation and modularity of skull and teeth in domesticated horses and wild equids. *Frontiers in Zoology*, 15, 14.

Klingenberg, C. P. (1996). Multivariate allometry. In L. F. Marcus, M. Corti, A. Loy, G. J. P. Naylor, & D. E. Slice (Eds.), *Advances in Morphometrics* (pp. 23–49). Plenum Press.

Klingenberg, C. P. (2014). Studying morphological integration and modularity at multiple levels: Concepts and analysis. *Philosophical Transactions of the Royal Society B*, 369(1649), 20130249. https://doi.org/10.1098/rstb.2013.0249

Klingenberg, C. P. (2021). How exactly did the nose get that long? A critical rethinking of the Pinocchio effect and how shape changes relate to landmarks. *Evolutionary Biology*, 48, 115–127.

Klingenberg, C. P., Barluenga, M., & Meyer, A. (2002). Shape analysis of symmetric structures: Quantifying variation among individuals and asymmetry. *Evolution*, 56(10), 1909–1920. https://doi.org/10.1111/j.0014-3820.2002.tb00117.x

Klingenberg, C. P., & Marugan-Lobon, J. (2013). Evolutionary covariation in geometric morphometric data: Analyzing integration, modularity, and allometry in a phylogenetic context. *Systematic Biology*, 62(4), 591–610. https://doi.org/10.1093/sysbio/syt025

Klingenberg, C. P., & Zimmermann, M. (1992). Static, ontogenetic, and evolutionary allometry: A multivariate comparison in nine species of water striders. *American Naturalist*, 140(4), 601–620. https://doi.org/10.1086/285430

Kraatz, B., Belabbas, R., Fostowicz-Frelik, L., Ge, D. -Y., Kuznetsov, A. N., Lang, M. M., López-Torres, S., Mohammadi, Z., Racicot, R.

A., Ravosa, M. J., Sharp, A. C., Sherratt, E., Silcox, M. T., Słowiak, J., Winkler, A. J., & Ruf, I. (2021). Lagomorpha as a model morphological system. *Frontiers in Ecology and Evolution*, 9, 636402.

Kraatz, B. P., & Sherratt, E. (2016). Evolutionary morphology of the rabbit skull. *PeerJ*, 4, e2453.

Kraatz, B. P., Sherratt, E., Bumacod, N., & Wedel, M. J. (2015). Ecological correlates to cranial morphology in leporids (Mammalia, Lagomorpha). *PeerJ*, 3, e844. https://doi.org/10.7717/peerj.844

Lande, R. (1980). The genetic covariance between characters maintained by pleiotropic mutations. *Genetics*, 94(1), 203–215. https://doi.org/10.1093/genetics/94.1.203

Leamy, L. & Atchley, W. (1984). Static and evolutionary allometry of osteometric traits in selected lines of rats. *Evolution*, 38, 47–54.

Linde-Medina, M., Boughner, J. C., Santana, S. E., & Diogo, R. (2016). Are more diverse parts of the mammalian skull more labile? *Ecology and Evolution*, 6(8), 2318–2324. https://doi.org/10.1002/ece3.2046

Machado, F. A., Hubbe, A., Melo, D., Porto, A., & Marroig, G. (2019). Measuring the magnitude of morphological integration: The effect of differences in morphometric representations and the inclusion of size. *Evolution*, 73(12), 2518–2528. https://doi.org/10.1111/evo.13864

Machado, F. A., Zahn, T. M. G., & Marroig, G. (2018). Evolution of morphological integration in the skull of Carnivora (Mammalia): Changes in Canidae lead to increased evolutionary potential of facial traits. *Evolution*, 111(489), 421. https://doi.org/10.1111/evo.13495

Marcus, L. F., Hingst-Zaher, E., & Zaher, H. (2000). Application of landmark morphometrics to skulls representing the orders of living mammals. *Hystrix*, 11, 27–47.

Marcy, A. E., Guillerme, T., Sherratt, E., Rowe, K. C., Phillips, M. J., & Weisbecker, V. (2020). Australian rodents reveal conserved cranial evolutionary allometry across 10 million years of murid evolution. *The American Naturalist*, 196, 755–768.

Marroig, G., & Cheverud, J. M. (2005). Size as a line of least evolutionary resistance: Diet and adaptive morphological radiation in new world monkeys. *Evolution*, 59(5), 1128–1142.

Marroig, G., & Cheverud, J. (2010). Size as a line of least resistance II: Direct selection on size or correlated response due to constraints? *Evolution*, 64(5), 1470–1488. https://doi.org/10.1111/j.1558-5646.2009.00920.x

Marroig, G., Shirai, L. T., Porto, A., de Oliveira, F. B., & De Conto, V. (2009). The evolution of modularity in the mammalian skull II: Evolutionary consequences. *Evolutionary Biology*, 36(1), 136–148. https://doi.org/10.1007/s11692-009-9051-1

Marshall, A. F., Bardua, C., Gower, D. J., Wilkinson, M., Sherratt, E., & Goswami, A. (2019). High-density three-dimensional morphometric analyses support conserved static (intraspecific) modularity in caecilian (Amphibia: Gymnophiona) crania. *Biological Journal of the Linnean Society*, 126(4), 721–742. https://doi.org/10.1093/biolinnean/blz001

Matthee, C. A., van Vuuren, B. J., Bell, D., & Robinson, T. J. (2004). A molecular supermatrix of the rabbits and hares (Leporidae) allows for the identification of five intercontinental exchanges during the Miocene. *Systematic Biology*, 53(3), 433–447. https://doi.org/10.1080/10635150490445715

Melo-Ferreira, J., Boursot, P., Carneiro, M., Esteves, P. J., Farelo, L., & Alves, P. C. (2012). Recurrent introgression of mitochondrial DNA among hares (*Lepus* spp.) revealed by species-tree inference and coalescent simulations. *Systematic Biology*, 61(3), 367–381. https://doi.org/10.1093/sysbio/syr114

Menegaz, R. A., Sublett, S. V., Figueroa, S. D., Hoffman, T. J., & Ravosa, M. J. (2009). Phenotypic plasticity and function of the hard palate in growing rabbits. *Anatomical Record*, 292(2), 277–284. https://doi.org/10.1002/ar.20840

Merriam, C. H. (1891). Results of a biological reconnoissance of Idaho, south of latitude 45° and east of the thirty-eighth meridian, made during the summer of 1890, with annotated lists of the mammals and birds, and descriptions of new species. *North American Fauna*, 5(5), 1–30.

Monteiro, L. R. (1999). Multivariate regression models and geometric morphometrics: The search for causal factors in the analysis of shape. *Systematic Biology*, 48(1), 192–199. https://doi.org/10.1080/106351599260526

Monteiro, L. R., Bonato, V., & Dos Reis, S. F. (2005). Evolutionary integration and morphological diversification in complex morphological structures: Mandible shape divergence in spiny rats (Rodentia, Echimyidae). *Evolution and Development*, 7(5), 429–439. https://doi.org/10.1111/j.1525-142X.2005.05047.x

Monteiro, L. R., & Nogueira, M. R. (2010). Adaptive radiations, ecological specialization, and the evolutionary integration of complex morphological structures. *Evolution*, 64(3), 724–744. https://doi.org/10.1111/j.1558-5646.2009.00857.x

Mossey, P. A. (1999). The heritability of malocclusion: Part 2. The influence of genetics in malocclusion. *British Journal of Orthodontics*, 26(3), 195–203. https://doi.org/10.1093/ortho/26.3.195

Neaux, D., Sansalone, G., Ledogar, J. A., Ledogar, S. H., Luk, T. H. Y., & Wroe, S. (2018). Basicranium and face: Assessing the impact of morphological integration on primate evolution. *Journal of Human Evolution*, 118, 43–55.

Nijhout, H. F. (2011). Dependence of morphometric allometries on the growth kinetics of body parts. *Journal of Theoretical Biology*, 288, 35–43. https://doi.org/10.1016/j.jtbi.2011.08.008

Oksanen, J., Guillaume Blanchet, F., Friendly, M., Kindt, R., Legendre, P., McGlinn, D., Minchin, P. R., O'Hara, R. B., Simpson, G. L., Solymos, P., Henry, M., Stevens, H., Szoecs, E., & Wagner, H. (2022). *vegan: Community ecology package. R package version 2.4-0*.

Olson, E. C., & Miller, R. L. 1958. *Morphological integration*. University of Chicago Press.

Paradis, E., Claude, J., & Strimmer, K. (2004). APE: Analyses of phylogenetics and evolution in R language. *Bioinformatics*, 20(2), 289–290. https://doi.org/10.1093/bioinformatics/btg412

Parsons, K. J., Son, Y. H., Crespel, A., Thambithurai, D., Killen, S., Harris, M. P., & Albertson, R. C. (2018). Conserved but flexible modularity in the zebrafish skull: Implications for craniofacial evolvability. *Proceedings of the Royal Society of London. Series B*, 285, 20172671.

Pavlicev, M., Cheverud, J. M., & Wagner, G. P. (2009). Measuring morphological integration using eigenvalue variance. *Evolutionary Biology*, 36(1), 157–170. https://doi.org/10.1007/s11692-008-9042-7

Peacock, D., & Abbott, I. (2013). The role of quoll (*Dasyurus*) predation in the outcome of pre-1900 introductions of rabbits (*Oryctolagus cuniculus*) to the mainland and islands of Australia. *Australian Journal of Zoology*, 61(3), 206–275. https://doi.org/10.1071/zo12129

Pelabon, C., Firmat, C., Bolstad, G. H., Voje, K. L., Houle, D., Cassara, J., Rouzic, A. L., & Hansen, T. F. (2014). Evolution of morphological allometry. *Annals of the New York Academy of Sciences*, 1320(58), 58–75. https://doi.org/10.1111/nyas.12470

Porto, A., Oliveira, F. de, Shirai, L., De Conto, V., & Marroig, G. (2009). The evolution of modularity in the mammalian skull I: Morphological integration patterns and magnitudes. *Evolutionary Biology*, 36, 118–135.

Porto, A., Shirai, L. T., de Oliveira, F. B., & Marroig, G. (2013). Size variation, growth strategies, and the evolution of modularity in the mammalian skull. *Evolution*, 67(11), 3305–3322. https://doi.org/10.1111/evo.12177

Pucciarelli, H. M., Dressino, V., & Niveiro, M. H. (1990). Changes in skull components of the squirrel monkey evoked by growth and nutrition: An experimental study. *American Journal of Physical Anthropology*, 81(4), 535–543. https://doi.org/10.1002/ajpa.1330810409

R Development Core Team. (2022). *R: A language and environment for statistical computing*. Vienna, Austria. http://www.R-project.org

Raidan, C., Costa, B. M. D., Marroig, G., Assis, A. P. A., & Paresque, R. (2021). Morphological integration and cranial modularity in six genera of echimyid rodents (Rodentia: Echimyidae). *Journal of Mammalogy*, 103, 648–662.

Randau, M., Sanfelice, D., & Goswami, A. (2019). Shifts in cranial integration associated with ecological specialization in pinnipeds (Mammalia, Carnivora). *Royal Society Open Science*, 6(3), 190201. https://doi.org/10.1098/rsos.190201

Revell, L. J. (2012). phytools: An R package for phylogenetic comparative biology (and other things). *Methods in Ecology and Evolution*, 3, 217–223.

Rhoda, D., Polly, P. D., Raxworthy, C., & Segall, M. (2021). Morphological integration and modularity in the hyperkinetic feeding system of aquatic-foraging snakes. *Evolution*, 75(1), 56–72. https://doi.org/10.1111/evo.14130

Rohlf, F. J., & Corti, M. (2000). Use of two-block partial least-squares to study covariation in shape. *Systematic Biology*, 49(4), 740–753. https://doi.org/10.1080/106351500750049806

Rohlf, F. J., & Slice, D. (1990). Extensions of the Procrustes method for the optimal superimposition of landmarks. *Systematic Zoology*, 39(1), 40–59. https://doi.org/10.2307/2992207

Sanger, T. J., Mahler, D. L., Abzhanov, A., & Losos, J. B. (2012). Roles for modularity and constraint in the evolution of cranial diversity among *Anolis* lizards. *Evolution*, 66(5), 1525–1542. https://doi.org/10.1111/j.1558-5646.2011.01519.x

Singh, N., Harvati, K., Hublin, J. -J., & Klingenberg, C. P. (2011). Morphological evolution through integration: A quantitative study of cranial integration in *Homo*, *Pan*, *Gorilla* and *Pongo*. *Journal of Human Evolution*, 62, 155–164.

Stott, P. (2015). Factors influencing the importation and establishment in Australia of the European hare (*Lepus europaeus*). *Australian Journal of Zoology*, 63(1), 46–75. https://doi.org/10.1071/zo14037

Suchentrunk, F., Slimen, H. B., & Sert, H. (2008). Phylogenetic aspects of nuclear and mitochondrial gene-pool characteristics of south and North African cape hares (*Lepus capensis*) and European hares (*Lepus europaeus*). *Lagomorph biology* (pp. 65–85). Springer.

Urošević, A., Ljubisavljević, K., & Ivanović, A. (2018). Multilevel assessment of the lacertid lizard cranial modularity. *Journal of Zoological Systematics and Evolutionary Research*, 57(1), 145–158. https://doi.org/10.1111/jzs.12245

Usui, K., & Tokita, M. (2018). Creating diversity in mammalian facial morphology: A review of potential developmental mechanisms. *EvoDevo*, 9, 15. https://doi.org/10.1186/s13227-018-0103-4

Voje, K. L., Hansen, T. F., Egset, C. K., Bolstad, G. H., & Pelabon, C. (2014). Allometric constraints and the evolution of allometry. *Evolution*, 68, 866–885.

Watanabe, A., Fabre, A. -C., Felice, R. N., Maisano, J. A., Müller, J., Herrel, A., & Goswami, A. (2019). Ecomorphological diversification in squamates from conserved pattern of cranial integration. *Proceedings of the National Academy of Sciences*, 116(29), 14688–14697. https://doi.org/10.1073/pnas.1820967116

Willmore, K. E., Leamy, L., & Hallgrímsson, B. (2006). Effects of developmental and functional interactions on mouse cranial variability through late ontogeny. *Evolution and Development*, 8(6), 550–567. https://doi.org/10.1111/j.1525-142X.2006.00127.x

Wilson, L. A. B. (2013). Allometric disparity in rodent evolution. *Ecology and Evolution*, 3(4), 971–984. https://doi.org/10.1002/ece3.521

Young, R. L., & Badyaev, A. V. (2006). Evolutionary persistence of phenotypic integration: Influence of developmental and functional relationships on complex trait evolution. *Evolution*, 60(6), 1291–1299.

Zelditch, M. L., & Goswami, A. (2021). What does modularity mean? *Evolution and Development*, 23(5), 377–403. https://doi.org/10.1111/ede.12390

Zelditch, M. L., & Swiderski, D. L. (2022). The predictable complexity of evolutionary allometry. *Evolutionary Biology*, 50, 56–77.

Zelditch, M. L., Swiderski, D. L., & Sheets, H. D. (2012). *Geometric morphometrics for biologists: A primer*. Elsevier.